

Agnieszka TOMAKA<sup>\*</sup>, Sylwia TRZESZKOWSKA-ROTKEGEL<sup>\*\*</sup>,  
Michał TARNAWSKI<sup>\*\*\*</sup>

## **CORRECTION OF ERROR IN 3D RECONSTRUCTION INDUCED BY CT GANTRY TILT**

The paper presents the problems connected with 3D reconstruction of CT slices of the database of orthodontic patients, using the commercial application software. Serious errors occurred for scans taken with a tilted CT gantry and inverse table movement. A compensation of the errors is proposed and the results after the compensation are verified by comparison to laser scans for a reference object, and to the measurements performed using the dedicated software of the CT station for selected cases in the database.

### **1. INTRODUCTION**

The development of modern CT modalities is accompanied by a reduction of patient exposure to X rays. Therefore CT imaging becomes a powerful diagnostic tool not only in the cases requiring surgical intervention. However, the software of graphics stations connected with CT machines remains in the hands of radiologists, and, for various reasons, is not fully accessible to other specialties. There still exists a need for systems which would put the potential of 3D imaging directly at the disposal of other practitioners.

The main example, which also inspired the present work, is the use of 3D reconstruction for the purposes of orthodontics. Traditional orthodontic diagnosis is based on cephalograms – planar X-ray projections of the patient's head placed in a cephalostat. Landmarks localization, the quantities to be measured, and the norms are well defined for 2D analyzes. But extending these analyzes to 3D is not straightforward and requires a special system which enables the expert to define his landmarks, measurements, and statistics.

To implement such an application we would have to repeat the work already done in CT software: read DICOM files, threshold the images, reconstruct 3D surfaces. The present work describes our experience with procedures of 3D surface reconstruction found in a commercial 3D application software. We purchased this software for a number of purposes, and one of them was to verify our own procedures. The reason we present this experience is to caution those who work with 3D reconstruction from CT images that even high-end commercial software systems can produce serious reconstruction errors.

We show situations when the errors appear and suggest a technique to compensate them. Next we verify our results by comparing the CT-based 3D reconstructions to laser scans, and by comparing the measurements taken from the reconstructions to measurements carried out using the dedicated software of the CT station.

### **2. 3D RECONSTRUCTION OF THE DATABASE**

In order to simplify the creation of a prototype system for 3D orthodontic analysis, we implemented add-in functions for an existing commercial 3D application software. We chose to implement add-ins instead of a full standalone application so as to use reconstruction procedures and mesh processing functions already present in the software, leaving for the future the choice of really necessary functions, which will have to be implemented in a standalone system.

#### **2.1. PRELIMINARY ACCURACY ESTIMATION**

To estimate the overall accuracy of the process of CT imaging and reconstruction we performed CT scanning (HiSpeed QX/i<sup>TM</sup>) of a reference object, which was a laboratory melting pot made of Si-Al-O-N ceramic. The reconstructed surfaces were then compared to laser scans of the object taken by the Konica Minolta VI-9i scanner. The object was chosen due to its regular cylindrical shape and good scanning properties: a matte surface not giving reflectance artifacts and gray colour easily seen by the scanner. Moreover, the ceramics having an X-ray attenuation coefficient lower than that of metals and comparable to the attenuation coefficient of bone doesn't produce artifacts which appear so often when medical protocols of CT scanning are applied to metal parts.

---

\* IITiS PAN,

\*\* Zakład Radiologii, ŚAM,

\*\*\* Stomatologia Rodzinna, B.M. Tarnawscy

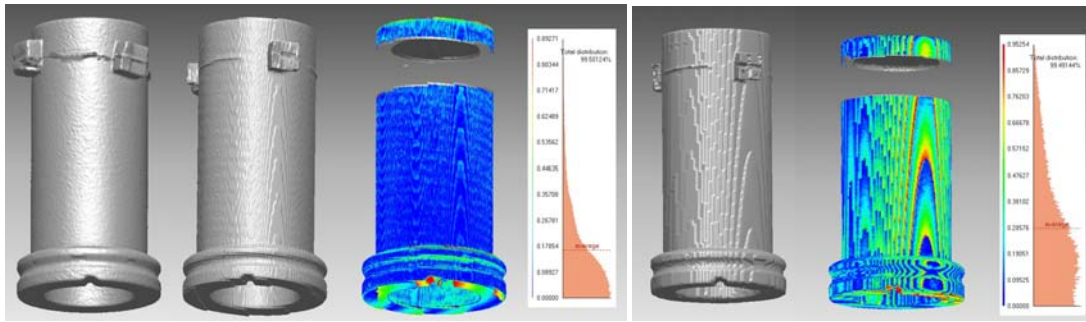


Fig. 1 Comparison of 3D reconstructions from CT and laser scans of reference object. From left: laser scan, 3D reconstruction for the object lying (parallel) during CT exam., distance map (CT-laser), object standing (perpendicular) during CT exam and its distance map.

The tests were performed with the long axis of the cylinder either parallel or perpendicular to the z axis (the direction of table movement). Additionally, we analyzed the influence of the inter-slice distance on the quality of reconstruction. The surface reconstructed from the CT scan was aligned with the 3D image acquired by the laser scanner. The root of the mean square distance (RMSD) between the nearest points of the two surface meshes was taken as the measure of reconstruction quality. (Fig 1.)

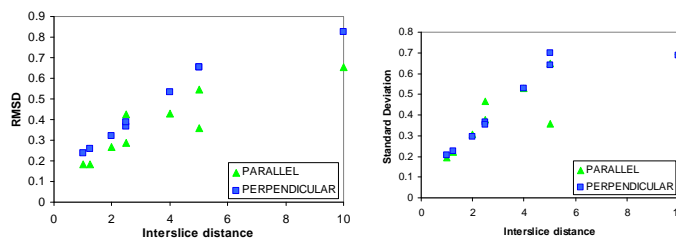


Fig2. The influence of inter-slice distance on the quality of reconstruction

The first conclusions were that the accuracy depends on the inter-slice distance and on the pixel size (Fig.2). Increasing inter-slice distance also increased the standard deviation. The standard deviation was approximately independent on object orientation. Moreover, the distance maps (Fig 1.) show errors in the area of the spurious edges caused by stair-shaped surfaces yielded by the reconstruction algorithms. Surface parts whose normals coincide with the movement direction are much more error-prone than others. The results were similar to those presented in [1]

## 2.2. DESCRIPTION OF A PROBLEM

After estimating the accuracy of 3D reconstruction, and finding it sufficient for orthodontic analyzes, we performed the reconstruction of the database of orthodontic patients using the commercial application software mentioned above, and simultaneously localized landmarks using our add-in function.

At first the error was not obviously noticeable because the data referred to patients with malformations, which could account for the strange appearance of the reconstructions. The first warning sign was the comparison of two sets of data for same patient. (Fig. 3) The reconstructed skull was unnaturally extended in the direction of the cranial base.

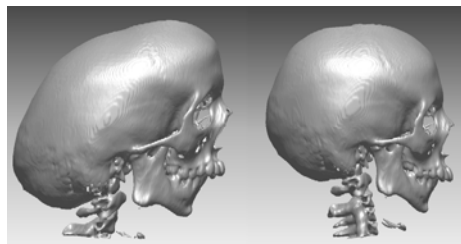


Fig 3. Reconstructions of two individual CT imaging of the same patient (#157)

The reason of such differences was not clear for us but we found that the commercial software had some reconstruction errors. In order to validate the whole set of reconstructions for each patient (if it was possible) we used imagery data from other

modalities to compare the shape of the skull. Comparison with cephalograms shows that this problem is not limited to one patient but concerns many (although not all) cases of data sets. (Fig 4)



Fig 4. Comparison of 3D reconstruction from CT with cephalograms (#3 gantry 12°) and (#187 gantry -18.5°)

Additionally, we compare the CT reconstruction of the skin with laser scans of the patient’s face, finding that some reconstructions had undergone a mirror transformation (Fig. 5)

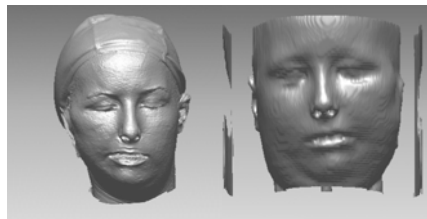


Fig 5. Comparison of laser scans and CT-based 3D reconstruction (#102)

The comparison of the results of reconstruction and our preliminary accuracy test lead to the conclusion that the test was performed for some particular conditions for with the accuracy was so high and should be performed again.

### 3. THE PROPERTIES OF CT IMAGING AND 3D RECONSTRUCTION

Image formation in CT examination relies on multiple projections of the patient taken as the X-ray source rotates around the patient. These projections are then processed using various methods (the Radon transform, FFT, filtered back projection, numeric methods) to reconstruct the 2D distribution of the attenuation coefficient. The method applied depends on the generation of the CT machine, but as the computing task becomes more complicated, due to the introduction of spiral movement or cone beam projections, numeric methods become more popular. The attenuation coefficients are next mapped to intensities and the image of one slice (cross-section) is saved using the DICOM standard [2]. The table moves and successive slices are obtained. The reconstructed slices acquired along the z axis can be stacked into a volumetric image of the object.

The reconstruction algorithms threshold this volumetric image and then triangulate boundary voxels into a 3D surface, represented by a triangle mesh. There exist many algorithms for 3D reconstruction but two approaches can be distinguished: creating a set of contours for each slice prior to linking them into a 3D mesh, and algorithms providing subpixel accuracy through an interpolation within each voxel (Marching Cubes, Marching Tetrahedra)[3,4,5]. A common feature of these algorithms is that they operate on indexes of voxels (rather than physical coordinates), leaving the calibration of the reconstructed mesh for the next stages of processing.

The aim of the calibration is to transform the mesh from the abstract coordinate system defined by voxel indexes into a Reference Coordinate System (RCS) connected with the patient. Calibration requires a knowledge of geometrical parameters of the CT scanning process, which also are stored in Dicom files [2].

(0018,0050)	Slice Thickness
(0018,1120)	Gantry/Detector Tilt
(0018,1121)	Gantry/Detector Slew
(0020,0032)	Image Position (Patient) (upper left hand corner, centre of the first voxel)
(0020,0037)	Image Orientation (Patient) The direction cosines of the first row and the first column with respect to the patient.
(0020,1041)	Slice Location Relative position of exposure expressed in mm
(0028,0030)	Pixel Spacing Physical distance in the patient between the centre of each pixel, specified by a numeric pair - adjacent row spacing and adjacent column spacing in mm

DICOM Documentation specifies for each slice (frame) the mapping of pixel location (i,j) to the RCS (Reference Coordinate System) as follows:

$$\begin{bmatrix} P_x \\ P_y \\ P_z \\ 1 \end{bmatrix} = \begin{bmatrix} X_x \Delta_i & Y_x \Delta_j & 0 & S_x \\ X_y \Delta_i & Y_y \Delta_j & 0 & S_y \\ X_z \Delta_i & Y_z \Delta_j & 0 & S_z \\ 0 & 0 & 0 & 1 \end{bmatrix} \begin{bmatrix} i \\ j \\ 0 \\ 1 \end{bmatrix} \quad (1)$$

Where:

$P_{xyz}$  – the coordinates of the voxel (i,j) in the frame's image plane in units of mm.

$S_{xyz}$  – the three values of the Image Position (Patient) (0020,0032) attributes. It is the location in mm from the origin of the RCS.

$X_{xyz}$  The values from the row (X) direction cosine of the Image Orientation (Patient) (0020,0037) attribute.

$Y_{xyz}$  – The values from the column (Y) direction cosine of the Image Orientation (Patient) (0020,0037) attribute.

i – Column index to the image plane. The first column is index zero.

$\Delta_i$  – Column pixel resolution of the Pixel Spacing (0028,0030) attribute in units of mm.

j – Row index to the image plane. The first row index is zero.

$\Delta_j$  – Row pixel resolution of the Pixel Spacing (0028,0030) attribute in units of mm.

Assuming  $S_x, S_y$  constants, and  $S_z$  as a function of image number k.

$$S_z(k) = S_z(k-1) + \Delta_k = S_z(0) + \Delta_k \cdot k$$

The mapping for a voxel image can be rewritten as follows:

$$\begin{bmatrix} P_x \\ P_y \\ P_z \\ 1 \end{bmatrix} = \begin{bmatrix} X_x \Delta_i & Y_x \Delta_j & 0 & S_x(0) \\ X_y \Delta_i & Y_y \Delta_j & 0 & S_y(0) \\ X_z \Delta_i & Y_z \Delta_j & \Delta_k & S_z(0) \\ 0 & 0 & 0 & 1 \end{bmatrix} \begin{bmatrix} i \\ j \\ k \\ 1 \end{bmatrix} = \begin{bmatrix} 1 & 0 & 0 & S_x(0) \\ 0 & 1 & 0 & S_y(0) \\ 0 & 0 & 1 & S_z(0) \\ 0 & 0 & 0 & 1 \end{bmatrix} \begin{bmatrix} X_x & Y_x & 0 & 0 \\ X_y & Y_y & 0 & 0 \\ X_z & Y_z & 1 & 0 \\ 0 & 0 & 0 & 1 \end{bmatrix} \begin{bmatrix} \Delta_i & 0 & 0 & 0 \\ 0 & \Delta_j & 0 & 0 \\ 0 & 0 & \Delta_k & 0 \\ 0 & 0 & 0 & 1 \end{bmatrix} \begin{bmatrix} i \\ j \\ k \\ 1 \end{bmatrix} = \mathbf{T} \cdot \mathbf{A} \cdot \mathbf{S} \cdot \begin{bmatrix} i \\ j \\ k \\ 1 \end{bmatrix} \quad (2)$$

Where  $S_x(0), S_y(0), S_z(0)$  - pixel location for the first image ( $k=0$ ),  $\mathbf{T}$  – translation matrix,  $\mathbf{A}$  - transformation from the coordinate system of the gantry into the Reference Coordinate System,  $\mathbf{S}$ - scaling matrix.

## 4. COMPENSATION OF THE ERROR INDUCED BY GANTRY TILT

### 4.1. ERROR ESTIMATION

The formula (2) specifies the calibration and could be used to implement our own procedure. The reason we decided to perform compensation, instead of reconstructing again the whole data set with our own procedures, was that we would like to avoid repeating a vast amount of work on semi-automatic feature localization, which had already been done.

To establish the sources of the error, attributes of all patients were carefully analyzed. For each patient the gantry slew was 0, the gantry tilt was in the range (-18.5°+12°),  $\begin{bmatrix} X_x & X_y & X_z \end{bmatrix} = \begin{bmatrix} 1 & 0 & 0 \end{bmatrix}$  and  $\begin{bmatrix} Y_x & Y_y & Y_z \end{bmatrix}$  depended on gantry tilt,  $S_x, S_y$  were constant for each patient slice. The errors appeared when the gantry tilt was not zero. Such a situation is also described in [6] as a limitation of medical rapid prototyping technologies. The authors advise that gantry tilt should be avoided when acquiring 3D CT scans. They warn that sophisticated mathematical algorithms are required to successfully correct the data, because of the ambiguity of the sign of the gantry tilt. In fact, when we applied shear, supposing that only the skewing part of the transformation had been omitted, in some cases this seemed to solve the problem, but in others the errors were twice as large as in the original reconstruction (Fig. 6).

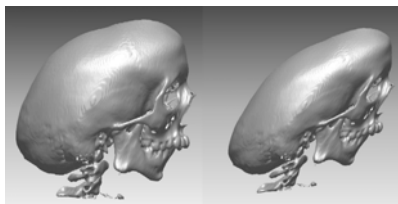


Fig. 6. Improper correction

We have noticed that our skewing correction either solved or aggravated the problem depending on direction of table travel, represented by the sign of  $\Delta_k$ . If  $\Delta_k < 0$  then the correction was successful. In the opposite case, the error increased.

Additionally, observations showed that all the reconstructions had their origin placed in (0,0,0) which meant that the Image Position (Patient) (0020,0032) attributes were not taken into account. The scaling in XY seemed to be exact (the pixel size attributes were applied). There was also an uncertainty which parameter was taken to calibrate Z axis. The observation showed that, when not chosen as the slice thickness, this parameter was equal to the module of the inter-slice distance. And this turned to be the reason of the mirror transformation which appears always when  $\Delta_k > 0$ . Summarizing, the 3D reconstruction that is performed by the commercial application is done in a coordinate system based on image indexes and then only rescaled using the pixel size attribute and absolute inter-slice distance, ignoring the direction of table movement.

To perform the correction, we had first to compensate the sign of  $\Delta_k$  of the scaling (matrix **S**), and then apply the shear (matrix **A**) and translation (matrix **T**) (using the symbols defined in the previous section).

#### 4.2. VERIFICATION

In order to verify the compensation we repeated the CT scanning of the melting pot using gantry tilt. For each orientation of the reference objects three examinations were done with gantry tilt equal to  $-11^\circ$ ,  $0^\circ$ ,  $10^\circ$ . The 3D reconstructions were performed (Fig. 7), next the compensation was applied and the results were compared to the surface obtained using a laser scanner. In this case the RMSD was less then 0.4 mm, although the max distance was a little larger than in the case without gantry tilt (Fig. 8).

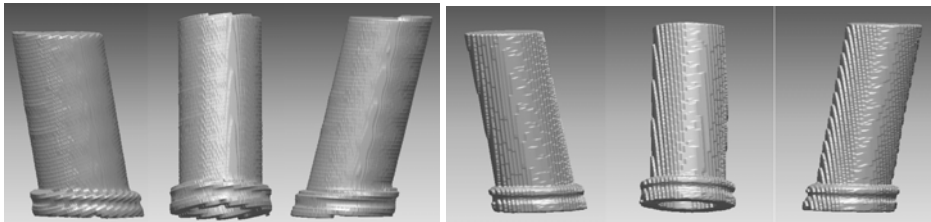


Fig. 7. 3D reconstructions of CT scans of the reference object

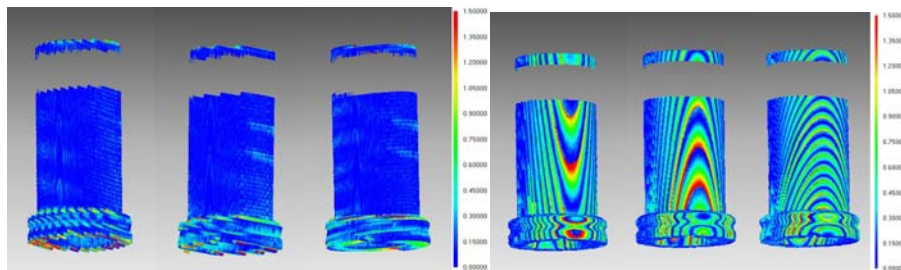


Fig. 8. The distance maps for the compensated 3D reconstruction to the laser scans.

Next we performed the compensation for those patients for whom other imagery data was available. The comparison of 3D reconstructions of two sets of the same patient from (Fig. 3) yielded a RMSD of about 0.25 mm (Fig. 9). Visual observation of the skull shapes from (Fig 4) showed that both images (3D CT reconstruction and cephalogram) could be obtained from the same patient (Fig. 10).

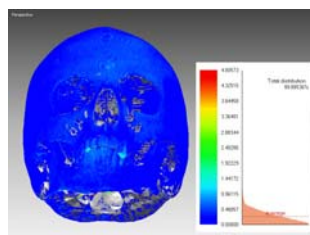


Fig. 9. Comparison of 3D reconstructions(after compensation) from two sets of data for the same patient.



Fig. 10. Comparisons of compensated 3D reconstr. with cephalograms (#3, gantry +12°), (#187 gantry -18.5°)

To obtain the quantitative measure of the accuracy of the compensation we compared 3D reconstructions for chosen patients by measuring, in each reconstruction, the distances between the same features – localized in uncompensated 3D reconstructions, then measured after applying the compensation and finally localized by a radiologist on the CT graphic station. We examined some measurements in the sagittal plane (N-Me, Me-Occ, N-Occ or ANS-Occ, ANS-Me, where N not available) and some other measurements (Me-JR Me-JL, JR-JL ).

	RMSD before compensation[mm]	Max difference before comp.[mm]	RMSD after compensation[mm]	Max difference after comp.[mm]
Jl-Me	8.19	15.64	0.73	1.25
Jr-Me	8.06	15.34	0.59	0.89
Jr-Jl	0.65	1.26	0.61	1.04
N-ANS	2.84	5.64	0.99	1.67
OCC-N	11.87	<b>30.19</b>	0.82	1.83
OCC-Me	13.18	21.70	0.62	1.08
OCC-ANS	8.96	16.35	0.72	1.64
Me-N	13.99	22.39	0.73	1.39
Me-ANS	8.79	14.31	0.59	0.99

The table shows the mean and maximum differences between the measurements taken in uncompensated 3D reconstruction and measurements on the CT graphics station (column 2 and 3) and the same differences after the compensation (columns 4,5). After the compensation the mean differences of the all measurements are less than 1 mm. The maximum differences reached 1.9 mm. However, it must be taken into account that there was no possibility to export landmarks position from the CT graphics station, and each measurement required a separate landmark localization. The error of the localization can then influence the overall accuracy. The amount of error in the uncompensated sets depends highly on the direction of the line along which the measurement was taken. The greatest error occurred in the OCC- N direction (more or less parallel to the cranial – base), the smallest in the Jr-Jl direction, more or less parallel to the X axis. In one case, the error was about 3cm, which is quite a big error that can seriously influence therapeutic decisions.

## 5. CONCLUSIONS

The paper was written to caution those who work with 3D reconstruction from CT images that even high-end commercial software systems can produce serious reconstruction errors. The error depends on gantry tilt and on the direction of the segment which is being measured. Bigger values of gantry tilt introduce greater errors, however, those errors are more likely to be noticed. A small gantry tilt does not deform the image to an extent that would be visible at first glance, but the measurements can be biased. Therefore, even having a high-end software system, the user should always verify the correctness of the 3D reconstruction.

## BIBLIOGRAPHY

- [1] DELINGETTE H., et all. Accuracy evaluation of 3d reconstruction from ct-scan images for inspection of industrial parts. In CEPADUES Ed., editor, Proceedings on the Conference on Quality Control with Artificial Vision (QCAV'97), Le Creusot, France, May 1997
- [2] Digital Imaging and Communications in Medicine DICOM, part3 Information Object Definitions., National Electrical Manufacturers Association, USA 2004
- [3] LORENSON w., CLINE H., Marching cubes: A high resolution 3D surface construction algorithm, ACM SIGGRAPH Computer Graphics, Vol. 21, No. 44, pp 163-169, New York, 1987.

- [4] PAYNE B., TOGA A.. Surface mapping brain function on 3D models. *IEEE Computer Graphics and Applications*, 10(5):33–41, September 1990.
- [5] TREECE G., PRAGER R., GEE A., Regularised marching tetrahedra: improved iso-surface extraction, CUED/F-INFENG/TR 333, September 1998
- [6] WINDER J., BIBB R., Medical Rapid Prototyping Technologies: State of Art and Current Limitations for Application in Oral and Maxillofacial Surgery, *J Oral Maxillofac. Surg.* Vol. 63, pp1006-1015, 2005

